Boletim da Sociedade Astronômica Brasileira, **35**, no. 1, 183-187

Searching for metal-poor dwarf galaxies in the S-PLUS survey

M. Grossi[1], D. R. Gonçalves[1], A. Krabbe[2], V. Silva[1], A. Cortesi[1,3], & C. Mendes de Oliveira[2]

[1] Observatório do Valongo, UFRJ, Ladeira Pedro Antônio 43, Saúde, Rio de Janeiro, RJ, 20080-090, Brazil. e-mail: grossi@astro.ufrj.br
[2] Universidade de São Paulo, IAG, Rua do Mato 1225, Sao Paulo, SP, Brazil
[3] Instituto de Física, UFRJ

Abstract. Metallicity (Z) is a fundamental tracer of the evolutionary process of a galaxy. It depends upon several factors such as the star formation rate and the gas-mass fraction, but it also reflects the interplay between stellar feedback and the accretion of metal-poor gas from the intergalactic medium. Despite the expected large population of low-luminosity galaxies, the low-mass and low- metallicity regime is still relatively little studied among galactic populations. Because the properties of their interstellar medium resemble those of the fundamental building blocks of galaxies, finding such objects in the Local Universe and obtaining detailed investigations is extremely important to understand the early stages of galaxy evolution. We used the DR3 catalog of the Southern Photometric Local Universe Survey (S-PLUS) to select low-Z dwarf galaxy candidates based on color selection criteria typical of low-Z star-forming dwarf galaxies. Our final sample contains ∼50 candidates. Spectral energy distribution (SED) fitting of the 12 S-PLUS bands shows that the majority of the candidates are best-fitted by very low stellar metallicities (1/50 - 1/200 Solar). We obtained Gemini/GMOS long-slit follow-up observations for a pilot sample of galaxies to confirm whether these galaxies have indeed low metallicities. We present the general properties of our metal-poor dwarf galaxy candidates and the spectroscopic follow-up results.

Resumo. A metalicidade (Z) é um traçador fundamental do processo evolutivo de uma galáxia. Depende de vários fatores, como a taxa de formação de estrelas e a fração de massa de gás, mas também reflete a interação entre o feedback estelar e a acreção de gás do meio intergaláctico pobre em metais. Apesar da grande população esperada de galáxias de baixa luminosidade, o regime de baixa massa e baixa metalicidade ainda é relativamente pouco estudado entre as populações galácticas. Uma vez que as propriedades do seu meio interestelar assemelham-se aos dos blocos fundamentais de formação de galáxias, encontrar tais objetos no Universo Local e obter investigações detalhadas é extremamente importante para compreender os estágios iniciais da evolução de galáxias. Usamos o catálogo DR3 do levantamento Southern Photometric Local Universe Survey (S-PLUS) para selecionar candidatas a galáxias anãs de baixo Z com base em critérios de seleção de cores típicos de galáxias anãs com formação de estrelas e baixa metalicidade A nossa amostra final contém ∼50 candidatos. O ajuste da distribuição de energia espectral das 12 bandas do S-PLUS mostra que a maioria dos candidatos têm metalicidades estelares muito baixas (1/50 - 1/200 do valor solar). Obtivemos observaçs de acompanhamento espectroscópico de fenda longa com Gemini/GMOS-S de uma subamostra para confirmar se essas galáxias têm de fato baixas metalicidades. Apresentamos as propriedades gerais de nossas candidatas a galáxias anãs pobres em metais e os resultados do acompanhamento espectroscópico.

Keywords. Galaxies: dwarf – Galaxies: ISM – Galaxies: evolution

1. Introduction

Metallicity is a fundamental tracer of the evolutionary process of a galaxy (Lequeux et al. 1979; Tremonti et al. 2004). It depends upon several factors such as the star formation rate and the gas-mass fraction, but it also reflects the interplay between stellar feedback and the accretion of metal-poor gas from the intergalactic medium (Lilly et al. 2013; Peng & Maiolino 2014). Low-luminosity galaxies are less chemically evolved than more massive systems, likely because of a less efficient star formation activity and a higher fraction of metals lost in supernovae events (Guseva et al. 2009; McQuinn et al. 2015; Gonçalves 2019). However, despite the expected large population of low-luminosity galaxies, the low-mass and low-metallicity regime is still relatively little studied among the galactic populations. In the standard cosmological scenario dwarf galaxies play a crucial role in the hierarchical formation of structures, since the first objects to form and contribute, through mergers, to the growth of more massive systems were low-mass and metal-poor galaxies (Bovill & Ricotti 2009; Bromm & Yoshida 2011). Atek et al. (2023) have recently reported the discovery by JWST of eight SFGs at $z \sim 6-8$ with 12 + log(O/H) ∼ 7, approximately 2% the solar value and stellar masses of a few 10^7 $M_\odot$. Nearby gas-rich, low-metallicity dwarfs are expected to be analogous to such primitive galaxies both because of their low abundances of heavy elements and the presence of intense bursts of star formation (Bouwens et al. 2016). However, due to their low intrinsic luminosity, detailed investigations of these objects at great distances is extremely complex. Therefore, it is important to combine the most detailed observations of the closest analogous objects with those of younger and more distant galaxies.

Dwarf galaxies in the Local Universe can be studied in different galaxy environments, from large under-dense regions – the voids – to rich clusters (Grossi 2019). Dwarf galaxies in low-density regions often show peculiar gas morphology and kinematics, likely associated to external gas accretion, and they can experience strong bursts of star formation (Hoyle et al. 2012). The most metal-poor dwarfs in the Local Universe are found in such large underdense regions (Sánchez Almeida et al. 2016a).

Progress in identifying new metal-poor systems have been relatively slow. Identifying these faint galaxies requires that they are relatively nearby, and/or that they are experiencing a recent star formation episode. Recent studies targeting large areas of the sky only managed to detect a small number of metal-poor dwarf galaxies; to date < 100 star-forming dwarfs with metallicity below 1/10 solar are known in the Local Universe ($z \lesssim 0.02$;

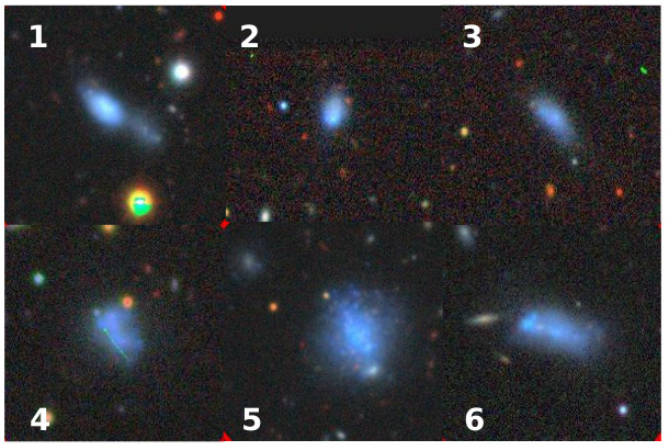

Figure 1. Legacy *grz* cutouts of the six metal-poor dwarf galaxy candidates selected in this work. Legacy images are deeper than S-PLUS allowing to infer more details about the galaxies morphology and structure. The cutout size is $40'' \times 40''$. See Table 1 for the definition of the ID numbers given at the top-left and bottom-left corners of each postage stamps.

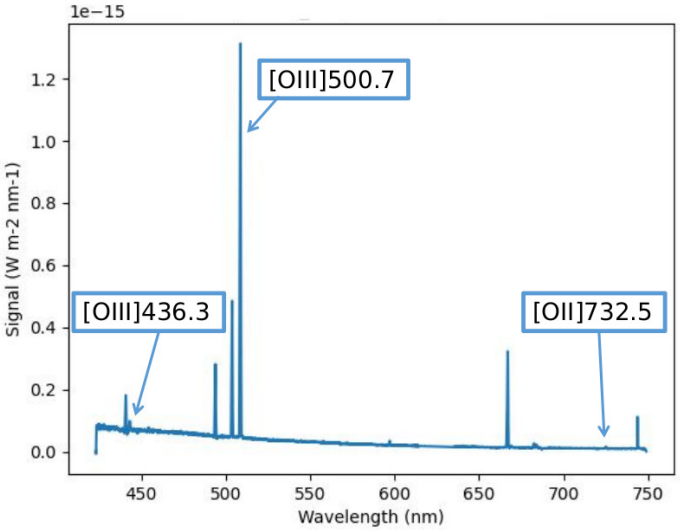

Figure 2. Gemini/GMOS-S spectra of SPLUSn14s01.030140 obtained with the B600 grating. The main [O III] and [O II] lines are highlighted.

Izotov et al. 2012; Hsyu et al. 2018; McQuinn et al. 2020; Lin et al. 2023).

The Southern Photometric Local Universe Survey (S-PLUS) is a 12-band optical survey conducted using the T80-South 0.826-m robotic telescope (T80S) located at Cerro Tololo Interamerican Observatory (Mendes de Oliveira et al. 2019). S-PLUS uses the Javalambre 12-band magnitude system (Cenarro et al. 2019), which includes the five *ugriz* broad-band and seven narrow-band filters centred on prominent stellar spectral features such as [OII]$\lambda\lambda\lambda$3727,3729, CaII H+K, Hδ, Hα, and the CaII triplet. We used the DR3 catalog of S-PLUS to select low-Z dwarf galaxies candidates. Following Hsyu et al. (2018, hereafter H18), we applied colour selection criteria typical of low-metallicity star-forming dwarf galaxies, such as IZw18 or Leo P. Our aim is to start building a sample of low-metallicity dwarf galaxy candidates in the southern hemisphere and to perform a spectroscopic follow-up campaign to confirm that they are poorly chemically evolved systems. Once we have constrained their abundances we can derive scaling relations and study their global properties in order to understand whether their low metallicity are due to either a slow secular evolution or to some external events related to their local environment. In these proceedings we present the preliminary results of our project within the S-PLUS collaboration.

2. Sample Selection

We searched for low-metallicity objects in the DR3 catalogue of S-PLUS applying colour selection criteria typical of low-metallicity star-forming dwarf galaxies. These colour cuts were defined in H18 from the analysis of galaxies in the SDSS survey:

$$0.2 \leq u - g \leq 0.6$$

$$-0.2 \leq g - r \leq 0.2$$

$$-0.7 \leq r - i \leq -0.1$$

$$-0.4 - 2\Delta z \leq i - z \leq 0.1\ .$$

Follow-up spectroscopic studies showed that ~45% of the galaxies selected with these color cuts in the SDSS had metallicities below 1/10 of the solar value and 6% have $Z \lesssim 5\%\ Z_{\odot}$ (H18).

We applied these criteria to the S-PLUS DR3 catalog (~ 200000 objects), for those objects with $r < 18$ mag. After visual inspection to reject spurious candidates we defined a final sample of 48 metal-poor dwarf galaxy candidates.

As a first test to confirm the metal-poor nature of our candidates we performed spectral energy distribution (SED) fitting of the 12 S-PLUS bands with the Code Investigating GALaxy Emission CIGALE (Boquien et al. 2019). We used a double exponential star formation history and we left the stellar metallicity as a free parameter, ranging between 1/200 $Z_{\odot}$ and 1 $Z_{\odot}$. The majority of the candidates (43 out of 48) have SEDs that are best-fitted by best stellar metallicity of Z = 0.0004 (1/50 Solar) or Z = 0.0001 (1/200 Solar). The stellar masses obtained from population synthesis models range between 10^7 and few times 10^9 $M_{\odot}$ and they are comparable to those obtained using the relation between $g - i$ colour and mass-to-light ratio derived by stellar population synthesis models (Bell et al. 2003, see Table 1). We started a pilot spectroscopic follow-up campaign between 2022 and 2023 with Gemini/GMOS South. Four objects were targeted in two different Fast Turnaround runs and two more galaxies have oxygen abundances derived with the direct method in the literature (see Table 1). We display the images of these six targets in Fig. 1. The images are taken from the DESI Legacy Imaging Surveys (Dey et al. 2019). Being deeper than S-PLUS, Legacy images allow us to better identify the morphology and structure of our targets.

3. Comparison samples

We compare our targets with metal-poor dwarf galaxies selected in the same way in other photometric surveys such as the SDSS (H18), and the Dark Energy Survey (DES; Lin et al. 2023, hereafter L23). The only difference between L23 and H18 is that $u-$band photometry is not available over the DES area, therefore, they modified the $u - g$ colour-cut criterion into a $NUV - g$ condition based on the GALEX NUV filter (Martin et al. 2005). We select only galaxies in both samples that have oxygen abundances derived with the direct method.

Table 1. Properties of the S-PLUS galaxies observed with GMOS (1-4) and with spectroscopic observations from previous studies (5-6).

	S-PLUS ID	RA	DEC	r [AB mag]	z_{spec}	log(M_*) [$M_\odot$]	12+log(O/H) [dex]
1	s27s07.015037	00:37:13.1	-35:08:48	16.79±0.01	0.0138	8.82	7.12±0.10
2	n14s01.030140	10:00:27.6	-17:28:25	17.54±0.02	0.0162	8.73	7.68±0.10
3	n13s01.028936	10:01:16.3	-16:13:49	17.76±0.03	0.0075	7.72	7.29±0.10
4	n02n27.053558	12:23:23.3	01:48:52	17.07±0.02	0.0067	7.76	7.46±0.10
5	s29s37.048546	04:05:20.4	-36:48:59	16.29±0.01	0.0027[a]	7.56	7.35±0.04[a]
6	n03s22.026437	11:57:12.0	-02:41:12	17.10±0.02	0.0046[b]	8.16	7.48±0.14[b]

[a] Guseva et al. (2009), [b] Sánchez Almeida et al. (2016b).

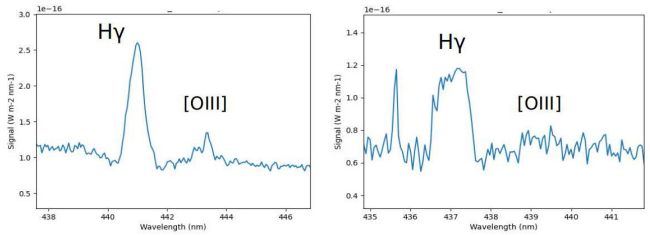

Figure 3. Example of GMOS spectra obtained with2 B600 gratings, (for two dwarf galaxies within our sample: n14s01.030140 (left panel), SPLUSn02n27.053558 (right panel). ´The figure shows that the [O III]λ4363 line is detected in the left panel, and it is not detected in the right panel.

4. Gemini/GMOS-S observations

The observations were carried out during two Fast Turnaround runs in 2022 and 2023 with the Gemini Multi-Object Spectrograph (GMOS) instrument (Hook et al. 2004) on the Gemini South Telescope (Program IDs GS-2022B-FT-210, GS-2023A-FT-204). We used the B600 grism with a 2″ slit width. The wavelength range covers between 4300 and 7500 Å with a central wavelength λ_c of 5300 Å. This choice allowed us to include all the major emission lines needed to determine the oxygen abundance with the direct method (see Fig, 2). The spectral resolution is R = 1688.The total integration time ranged between 1350 and 7200 seconds. The position of the longslit was defined according to the evidence of Hα emission in the S-PLUS images. Spectra of CuAr arc lamps were obtained for wavelength calibrations. Bias frames and dome flats were also obtained to correct for the detector bias level and pixel-to-pixel variations, respectively. The spectrophotometric standard LTT2415 was observed using the same experimental set-up.

For the first two runs we selected those targets that were best observable in semesters 2022B, 2023A and that were characterized by the lowest best-fit metallicities in our SED fitting analysis. The data were reduced using common procedures for longslit data from the Gemini GMOS Dragons package (Labrie et al. 2023).

Our aim is to derive the oxygen abundances using the direct method, which utilizes the flux ratio of auroral [O III]λ4363 to strong lines such as [OIII]$\lambda\lambda$4959,5007, to measure the electron temperature of the gas and infer the gas metallicity. Spectroscopic observations are fundamental to constrain our selection methods and confirm that we are building a sample of metal-poor dwarf galaxies. Strong-line calibrations have been widely applied to determine oxygen abundances at both low and high redshifts, but despite the convenience of this method, the relationship between strong line ratios and metallicity is complicated due to their sensitivity to the hardness of the incident stellar radiation field. For this reason estimates of the oxygen abundance through the direct method are considered to be more robust.

In Fig. 3 we display an inset of the spectra obtained for two objects. The figure shows that even with long exposures on a 8-meter telescope, the detection of the auroral line is challenging in these galaxies (right panel of Fig. 3).

5. Results

5.1. Oxygen abundances

We use the extinction-corrected emission line fluxes derived from the GMOS spectrum and the prescriptions of Magrini & Gonçalves (2009) to derive heavy element abundances in our galaxies. The electron temperature T_e [O III] is calculated from the [O III]λ4363/(λ4959 + λ5007) emission-line flux ratio and it is used to derive the abundances of O^{++}. The abundances of O^+ , N^+ and S^+ are derived assuming the empirical relation of Pagel et al. (1992) between the O^+ and O^{++} electron temperatures (T_e [O II], T_e [O III]). The electron number density is estimated from the [S II]λ6717/λ6731 flux ratio. Lastly we derived the total oxygen abundance as $O/H = O^+/H + O^{++}/H$. The oxygen auroral line was not detected in one object (SPLUSn02n27.053558). In this case we derived the metal abundance using the HII-CHImistry, a tool that calculates the oxygen abundance comparing emission-line intensities to grids of photoionization models (Pérez-Montero 2014). The abundances derived with this tool have been proved to be consistent with those based on the direct method (Pérez-Montero 2014).

5.2. Scaling relations

Once we estimate O/H we can derive scaling relations for these galaxies such as the mass-metallicity ($M-Z$) relation (Tremonti et al. 2004; Curti et al. 2020) and compare if they follow the general trend observed in galaxies of the local volume legacy (LVL) survey (Berg et al. 2012). Our sample of galaxies (stars in Fig. 4), as well as other objects from the comparison samples, appear to be offset from the main relation defined by the LVL (black line in Fig. 4). The presence of metal-poor outliers at a given stellar mass is in general attributed to external events. This can happen if star formation occurs in pockets of pristine gas accreted from the intergalactic medium (Sánchez Almeida et al. 2016a), or if it is triggered by a merger/interaction of a close galaxy pairs (Ellison et al. 2008; Lelli et al. 2012). In these scenarios, the metallicity of the ISM will be diluted and the galaxy would appear as an outlier in the $M-Z$ relation as well as in the

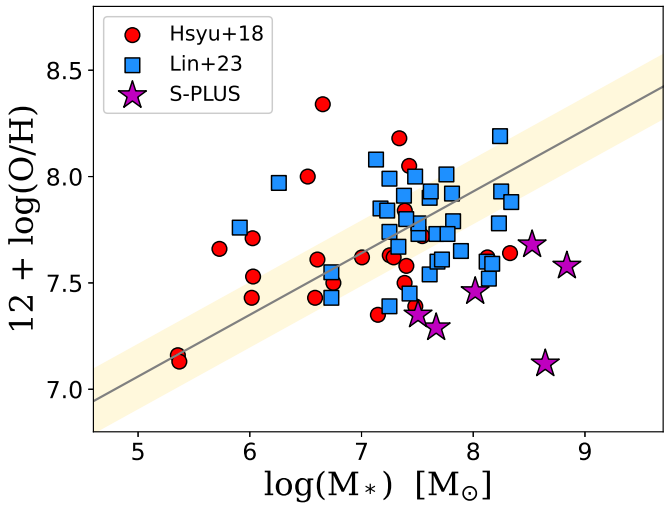

Figure 4. Mass-metallicity relation for a sample of dwarf galaxies selected in different photometric surveys (SDSS, DES, S-PLUS) using the same colour cuts discussed in the scientific justification. The galaxies are compared to the relation found in the Local Volume Legacy (LVL) survey (Berg et al. 2012, black line). The galaxies selected from the S-PLUS survey (purple stars) show a large offset from the main relation of the LVL galaxies. Stellar masess and oxygen abundances are derived in the same way in the three samples.

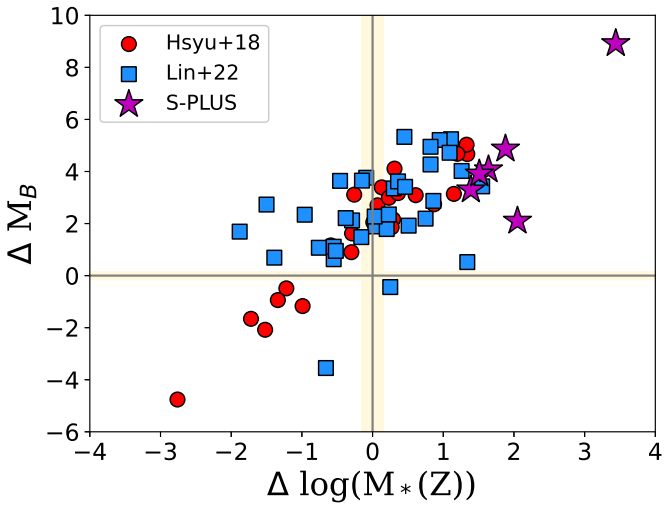

Figure 5. Offsets from the mass-metallicity (x axis) and from the luminosity metallicity relations for the sample of dwarf galaxies selected in different photometric surveys (SDSS, DES, S-PLUS). The offsets are calculate from the relation found in the Local Volume Legacy (LVL; Berg et al. 2012). The yellow shaded area shows the 1σ scatter of the $L-Z$ and $M-Z$ relatin in the LVL. The galaxies selected from S-PLUS (purple stars) show the largest offsets in both relations compared with the galaxies in the other surveys.

luminosity-metallicity ($L-Z$) relation. Such an effect would be even stronger in the $L-Z$ (Ekta & Chengalur 2010; McQuinn et al. 2020) due to the high luminosity of young massive stars and the contribution of strong emission lines, making the star-forming dwarfs brighter in the B band when compared to galaxies of similar mass with a lower star formation activity.

To better show the discrepancy in the $L-Z$, $M-Z$ relations we show in Fig. 5 the luminosity and stellar mass offsets of the three samples, defining the offsets as the horizontal distance of each object from the $M-Z$ and $L-Z$ relations defined by the LVL galaxies. Several galaxies from the L23 and H18 samples have small or negative scatter from the $M-Z$ relation, and larger scatter from the L–Z relation, with $\Delta L(Z)$ well above 1σ. However, almost half of the galaxies of both samples are located on the upper right side of the plot, with the S-PLUS galaxies being the most extreme outliers in both relations. S-PLUSs27s07.015037, the most metal-poor galaxy of our sample (see Tab. 1), is the most extreme outlier, lying at the top-right corner of Fig. 5. Among our six metal-poor targets, two galaxies, S-PLUSs27s07.015037 (1 in Fig. 1) and SPLUs29s37.048546 (5 in Fig. 1), seem to have a fainter nearby companion at a projected distance of 3 and 2 kpc, respectively (first two panels in the top row of Fig. 1). While in the first case the two systems appear to be in interaction, in the second case it is not clear from the Legacy image whether the faint galaxy is actually a companion or just a background object.

5.3. Optical morphologies

As a further test, we analysed the $r-$band images of our sample looking for evidence of perturbations that may give hints about galaxy galaxy interactions or mergers. We used `statmorph` (Rodriguez-Gomez et al. 2019) to calculate non-parametric morphological diagnostics such as the Gini coefficient (G), the second moment of the brightest pixels of a galaxy containing 20 per cent of the total flux (M_{20}; Lotz et al. 2004), and the concentration–asymmetry–smoothness system (CAS; see Conselice 2003, for details). These diagnostics have been extensively applied to quantify galaxy morphologies and to identify systems with signatures of recent or ongoing mergers. Particularly, the position of a galaxy in the $G-M_{20}$ plane allows us to separate major mergers from non-interacting galaxies (Lotz et al. 2004). Mergers occupy the region defined by the following relation: $S(G, M_{20}) = 0.14\ M_{20} + G - 0.33 > 0$ (Lotz et al. 2008, yellow line in Fig. 6). Only a few galaxies have $S > 0$ and lie in the merger region of the diagram but none of the objects that have been followed up with GMOS (although SPLUSn02n27.053558 lies at the very edge of the merger region, Fig. 6). However, this does not rule out that these galaxies might be experiencing minor merger events. Hoyos et al. (2012) report that in late minor mergers in which the less massive galaxies have been almost entirely dissolved the application of these diagnostics is less effective. Another possibility is that the stellar components have not been already remarkably disturbed by the interaction while the external gas component has been already stripped from the less massive companion and accreted by the main star forming system, as it occurs in IZw18 (Lelli et al. 2012). Lastly, if the star formation process is triggered by accretion from the intergalactic medium, the stellar disk will not be perturbed but the galaxies will appear as metal-poor outliers in the mass-metallicity relation (Sánchez Almeida et al. 2016a).

6. Summary and conclusions

We presented a selection of 48 star-forming dwarfs from the S-PLUS survey that are expected to have very metal-poor ISM based on their *ugriz* colours and SED fitting using the whole set of 12 filters provided by S-PLUS, 5 broad bands and 7 narrow bands. We just started a spectroscopic follow-up campaign with the Gemini/GMOS-S telescope to confirm their low metal

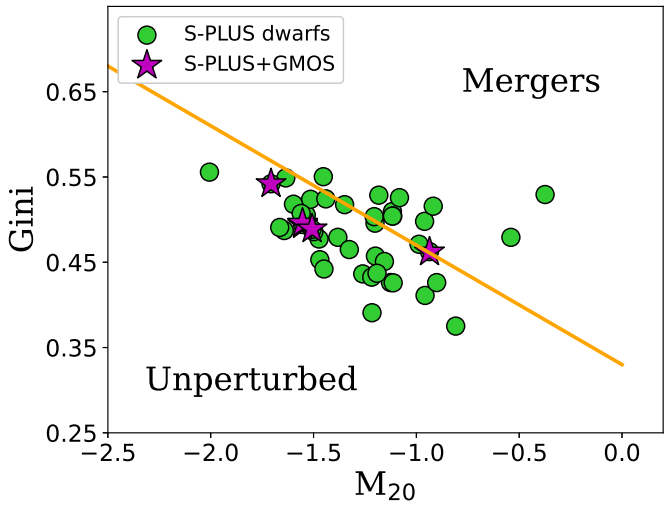

Figure 6. Gini-M_{20} diagram with our sample overlaid. High Gini and M_{20} values imply that a galaxy is in a merger phase. The yellow lines show the separation between mergers and non-interacting galaxies. Among the galaxies followed-up with GMOS, only one (SPLUSn02n27.053558) is slightly above the threshold values that separate major-merger candidates from non-interacting galaxies.

abundances and verifiy the photometric selection method that we applied. We observed four galaxies and derived O/H using the direct method in all but one galaxy (SPLUSn02n27.053558). We found oxygen abundances in the literature for two additional systems. All the objects appear to be very metal-poor galaxies, with 12 + log(O/H) < 7.65, i.e. lower than 1/10th of the solar abundance. Two dwarfs are extremely metal poor, with 12 + log(O/H) < 7.35, or less than 1/20th the solar abundance. We derived the $M-Z$ and $L-Z$ relations combining our targets with other samples of dwarf galaxies selected in the SDSS and DES surveys. The S-PLUS galaxies are the most extreme outliers in both relations. We suggest that an external event occurred, triggering star formation and lowering the oxygen abundance. Such an event might be associated to either gas accretion from the inter-galactic medium or an interaction with a companion. The six galaxies do not appear to have disturbed optical morphologies that might be related to a recent major merger event, according to their location in the Gini-M_{20} plot, however two systems present faint companions in the optical images within a few kpc project distance. High resolution images of the ionized and atomic gas will be needed to discriminate between the external gas accretion or galaxy-interaction scenarios. We plan to increase the sample of spectroscopically confirmed systems in the near future to assemble a statistically significant sample of metal-poor galaxies in the southern hemisphere and to investigate the role of the star formation rate in the deviation from the mass-metallicity relation (Mannucci et al. 2010; Curti et al. 2020).

Acknowledgements. MG acknowledges support from FAPERJ grant E-26/211.370/2021. DRG acknowledges FAPERJ (E-26/211.370/2021;E-26/211.527/2023) and CNPq (313016/2020-8) grants.

References

Atek, H., Labbé, I., Furtak, L. J., et al. 2023, arXiv e-prints, arXiv:2308.08540
Bell, E. F., McIntosh, D. H., Katz, N., & Weinberg, M. D. 2003, ApJS, 149, 289
Berg, D. A., Skillman, E. D., Marble, A. R., et al. 2012, ApJ, 754, 98
Boquien, M., Burgarella, D., Roehlly, Y., et al. 2019, A&A, 622, A103
Bouwens, R. J., Oesch, P. A., Labbé, I., et al. 2016, ApJ, 830, 67
Bovill, M. S., & Ricotti, M. 2009, ApJ, 693, 1859
Bromm, V., & Yoshida, N. 2011, ARA&A, 49, 373
Cenarro, A. J., Moles, M., Cristóbal-Hornillos, D., et al. 2019, A&A, 622, A176
Conselice, C. J. 2003, ApJS, 147, 1
Curti, M., Mannucci, F., Cresci, G., & Maiolino, R. 2020, MNRAS, 491, 944
Dey, A., Schlegel, D. J., Lang, D., et al. 2019, AJ, 157, 168
Ekta, B., & Chengalur, J. N. 2010, MNRAS, 406, 1238
Ellison, S. L., Patton, D. R., Simard, L., & McConnachie, A. W. 2008, AJ, 135, 1877
Gonçalves, D. R. 2019, in Dwarf Galaxies: From the Deep Universe to the Present, ed. K. B. W. McQuinn & S. Stierwalt, Vol. 344, 161–177
Grossi, M. 2019, in Dwarf Galaxies: From the Deep Universe to the Present, ed. K. B. W. McQuinn & S. Stierwalt, Vol. 344, 319–330
Guseva, N. G., Papaderos, P., Meyer, H. T., Izotov, Y. I., & Fricke, K. J. 2009, A&A, 505, 63
Hook, I. M., Jørgensen, I., Allington-Smith, J. R., et al. 2004, PASP, 116, 425
Hoyle, F., Vogeley, M. S., & Pan, D. 2012, MNRAS, 426, 3041
Hoyos, C., Aragón-Salamanca, A., Gray, M. E., et al. 2012, MNRAS, 419, 2703
Hsyu, T., Cooke, R. J., Prochaska, J. X., & Bolte, M. 2018, ApJ, 863, 134
Izotov, Y. I., Thuan, T. X., & Guseva, N. G. 2012, A&A, 546, A122
Labrie, K., Simpson, C., Cardenes, R., et al. 2023, Research Notes of the American Astronomical Society, 7, 214
Lelli, F., Verheijen, M., Fraternali, F., & Sancisi, R. 2012, A&A, 537, A72
Lequeux, J., Peimbert, M., Rayo, J. F., Serrano, A., & Torres-Peimbert, S. 1979, A&A, 80, 155
Lilly, S. J., Carollo, C. M., Pipino, A., Renzini, A., & Peng, Y. 2013, ApJ, 772, 119
Lin, Y.-H., Scarlata, C., Mehta, V., et al. 2023, ApJ, 951, 138
Lotz, J. M., Jonsson, P., Cox, T. J., & Primack, J. R. 2008, MNRAS, 391, 1137
Lotz, J. M., Primack, J., & Madau, P. 2004, AJ, 128, 163
Magrini, L., & Gonçalves, D. R. 2009, MNRAS, 398, 280
Mannucci, F., Cresci, G., Maiolino, R., Marconi, A., & Gnerucci, A. 2010, MNRAS, 408, 2115
Martin, D. C., Fanson, J., Schiminovich, D., et al. 2005, ApJ, 619, L1
McQuinn, K. B. W., Skillman, E. D., Dolphin, A., et al. 2015, ApJ, 815, L17
McQuinn, K. B. W., Berg, D. A., Skillman, E. D., et al. 2020, ApJ, 891, 181
Mendes de Oliveira, C., Ribeiro, T., Schoenell, W., et al. 2019, MNRAS, 489, 241
Pagel, B. E. J., Simonson, E. A., Terlevich, R. J., & Edmunds, M. G. 1992, MNRAS, 255, 325
Peng, Y.-j., & Maiolino, R. 2014, MNRAS, 438, 262
Pérez-Montero, E. 2014, MNRAS, 441, 2663
Rodriguez-Gomez, V., Snyder, G. F., Lotz, J. M., et al. 2019, MNRAS, 483, 4140
Sánchez Almeida, J., Elmegreen, B. G., Muñoz-Tuñón, C., & Elmegreen, D. M. 2016a, in The Zeldovich Universe: Genesis and Growth of the Cosmic Web, ed. R. van de Weygaert, S. Shandarin, E. Saar, & J. Einasto, Vol. 308, 390–393
Sánchez Almeida, J., Pérez-Montero, E., Morales-Luis, A. B., et al. 2016b, ApJ, 819, 110
Tremonti, C. A., Heckman, T. M., Kauffmann, G., et al. 2004, ApJ, 613, 898